nature medicine

Functional engraftment of colon epithelium expanded *in vitro* from a single adult Lgr5$^+$ stem cell

Shiro Yui[1,6], Tetsuya Nakamura[2,6], Toshiro Sato[3,5], Yasuhiro Nemoto[1], Tomohiro Mizutani[1], Xiu Zheng[1], Shizuko Ichinose[4], Takashi Nagaishi[1], Ryuichi Okamoto[2], Kiichiro Tsuchiya[1], Hans Clevers[3] & Mamoru Watanabe[1]

Adult stem-cell therapy holds promise for the treatment of gastrointestinal diseases. Here we describe methods for long-term expansion of colonic stem cells positive for leucine-rich repeat containing G protein-coupled receptor 5 (Lgr5$^+$ cells) in culture. To test the transplantability of these cells, we reintroduced cultured GFP$^+$ colon organoids into superficially damaged mouse colon. The transplanted donor cells readily integrated into the mouse colon, covering the area that lacked epithelium as a result of the introduced damage in recipient mice. At 4 weeks after transplantation, the donor-derived cells constituted a single-layered epithelium, which formed self-renewing crypts that were functionally and histologically normal. Moreover, we observed long-term (>6 months) engraftment with transplantation of organoids derived from a single Lgr5$^+$ colon stem cell after extensive *in vitro* expansion. These data show the feasibility of colon stem-cell therapy based on the *in vitro* expansion of a single adult colonic stem cell.

Epithelial stem cells maintain tissue homeostasis throughout the gastrointestinal tract[1–3]. The Wnt, bone morphogenetic protein (BMP) and Notch cascades function together to regulate stem-cell maintenance[4,5]. *Lgr5* marks stem cells in small intestinal and colonic crypts[6] and in gastric units[7]. *Bmi1* may mark distinct stem cells in the proximal small intestine[8]. It has been shown that freshly isolated intestinal epithelium can be transplanted in rodents after resident epithelium has been surgically removed[9,10]. We previously developed a three-dimensional culture technique that allows expansion of single Lgr5$^+$ stem cells from small intestine[11], stomach[7] and colon[12]. The resulting organoids then expand and self organize into an epithelial architecture that is reminiscent of that seen in *in vivo* histology. Moreover, the growing organoids maintain their tissue identity even after prolonged culture. Here we sought to evaluate whether the cultured Lgr5$^+$ cells faithfully represent the tissue-resident Lgr5$^+$ stem cells and, thus, are able to regenerate epithelial tissue *in vivo*. Considering that the colon is very vulnerable to disease in humans, we focused on colonic stem cells in our analyses.

RESULTS

Long-term, serum-free culture system for colonic organoids

We subjected the colons of adult mice to a combination of enzymes[13], reducing agents[14] and mechanical disruption. The resulting crypt fragments were mostly devoid of α smooth muscle actin gene (*Acta2*)-expression–positive non-epithelial components and consisted of a mix of cadherin 1, type 1, E-cadherin (*Cdh1*)$^+$ cells expressing terminal differentiation marker genes (*Muc2*, *CA2* and *ChgA*) and Lgr5$^+$ stem cells (**Supplementary Fig. 1a,b**).

The addition of R-spondin 1 (Rspo1), Noggin and epidermal growth factor (EGF), which are all essential to small intestine culture[11], did not maintain the growth of colonic crypts. We therefore developed the following 'TMDU (Tokyo Medical and Dental University) protocol': we embedded crypts in type I collagen in serum-free medium with Wnt3a, hepatocyte growth factor (HGF)[15,16] and BSA, in addition to Rspo1, Noggin and EGF (**Supplementary Fig. 1c**). Sequential imaging of the cultures revealed rapid growth of cystic structures (**Fig. 1a**). Wnt3a, Rspo1 and BSA were essential to this growth (**Supplementary Fig. 1d**). As predicted by previous results[17,18], Rspo1 could be substituted with Wnt3a (data not shown). Although Noggin, EGF and HGF were not essential for growth of the colonic crypts, each enhanced their growth (**Supplementary Fig. 1e**). The colonic organoids rarely had buds (**Fig. 1a**, **Supplementary Fig. 2a** and **Supplementary Video 1**). Of note, small intestinal organoids also generate cystic structures when Wnt3a is added to them[19].

The colonic organoids were single layered (**Supplementary Fig. 2b**), and all the cells within were positive for Cdh1 expression (**Fig. 1b**). The basal membranes of the organoids faced outward (**Fig. 1b**). Ki67$^+$ cells were present in the colonic organoids (**Fig. 1b**), as were alcian blue–positive goblet cells, chromogranin A (ChgA)$^+$ enteroendocrine cells, carbonic anhydrase II (CA2)$^+$ colonocytes and cytochrome c oxidase subunit I (COX1)$^+$ tuft cells[20] (**Fig. 1b**). Transmission electron microscopy revealed epithelial characteristics such as microvilli (**Fig. 1c**) and junctional complexes (**Fig. 1d**) in the organoids. However, stromal cells were absent (**Supplementary Fig. 2c**). Mitotic cells with condensed chromosomes were present in the organoids (**Fig. 1e**), and goblet cells (**Fig. 1f**) and enteroendocrine cells (**Fig. 1g**) could also be clearly detected.

[1]Department of Gastroenterology and Hepatology, Graduate School, Tokyo Medical and Dental University, Bunkyo-ku, Tokyo, Japan. [2]Department of Advanced Therapeutics for Gastrointestinal Diseases, Tokyo Medical and Dental University, Bunkyo-ku, Tokyo, Japan. [3]Hubrecht Institute and University Medical Centre, Utrecht, The Netherlands. [4]Research Center for Medical and Dental Sciences, Tokyo Medical and Dental University, Bunkyo-ku, Tokyo, Japan. [5]Present address: Department of Gastroenterology, Keio University School of Medicine, Shinjuku-ku, Tokyo, Japan. [6]These authors contributed equally to this work. Correspondence should be addressed to H.C. (h.clevers@hubrecht.eu) or M.W. (mamoru.gast@tmd.ac.jp).

Received 30 July 2011; accepted 29 November 2011; published online 11 March 2012; doi:10.1038/nm.2695

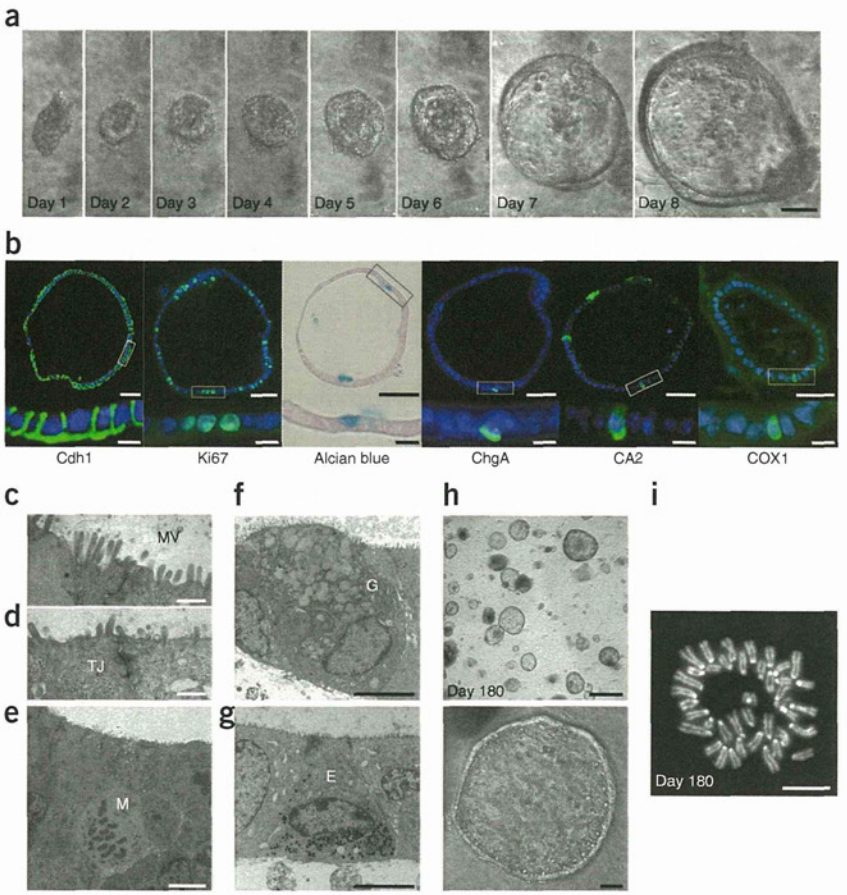

Figure 1 Long-term, serum-free culture of colonic epithelial cells. (**a**) A representative colonic crypt growing as a cystic structure. Scale bar, 50 μm. Time-lapse images of another colonic crypt are shown in **Supplementary Figure 2a** and **Supplementary Video 1**. (**b**) Histology of the colonic organoids at day 8 of culture. Cdh1$^+$ cells, actively proliferating Ki67$^+$ cells (green) and terminally differentiated cells stained with alcian blue (blue, goblet cells) or immunostained with ChgA (green, enteroendocrine cells), CA2 (green, colonocytes) or COX1 (green, tuft cells) are shown. Higher magnification views of the boxed areas are shown at the bottom. DAPI staining was performed, except for the experiments in which we performed alcian blue staining. Scale bars, top, 50 μm; bottom, 10 μm. (**c**–**g**) Transmission electron microscopy analysis for organoids at day 8. (**c**,**d**) Microvilli (MV) and intracellular tight junctions (TJ) are shown. (**e**) Mitotic (M) cells showing chromatin condensation. (**f**,**g**) Goblet cells (G) with mucus granules (**f**) and enteroendocrine cells (E) with electron dense granules (**g**) are shown. Scale bars: **c**,**d**, 0.5 μm; **e**–**g**, 5 μm. Low-power views of **f** and **g** are also shown in **Supplementary Figure 2c**. (**h**) The culture at day 180 (top) and its representative organoid (bottom). Scale bars, top, 500 μm; bottom, 50 μm. Images of the growth of a single cell after passage are shown in **Supplementary Figure 3** and **Supplementary Video 2**. (**i**) Metaphase spread of a cell at day 180 shows a normal karyotype ($2n = 40$). Scale bar, 10 μm.

The organoids could be passaged weekly at a 1:2 ratio (**Supplementary Fig. 3** and **Supplementary Video 2**). Addition of the Rho kinase inhibitor Y-27632 (ref. 21) improved the replating efficiency of the organoids[11]. We successfully propagated organoids for more than 6 months without clear alterations of morphology (**Fig. 1h**) or karyotype (**Fig. 1i**).

Lgr5$^+$ cells are enriched in colonic organoids

We tracked the expression of *Lgr5* over 60 d and found a substantial elevation during the first 8 d of observation (**Fig. 2a**). We found no change in the expression of *ChgA* and *CA2*, whereas *Muc2* expression was repressed in the first 8 d (**Fig. 2a**). Addition of a combination of Wnt3a, Rspo1 and BSA induced *Lgr5* expression (**Fig. 2b**). *Lgr5* expression was further upregulated by the addition of Noggin, which is an antagonist of BMP[22] (**Fig. 2b**). The Notch pathway suppresses the

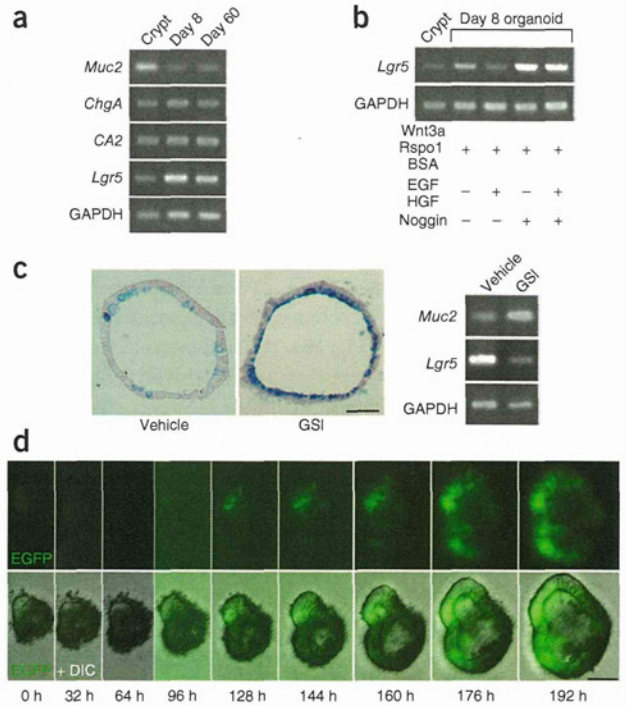

Figure 2 Lgr5$^+$ stem cells are enriched in cultured organoids. (**a**) RT-PCR analysis of the colonic crypts immediately after isolation (crypt) or organoids cultured for 8 or 60 d. *Lgr5* was upregulated and stayed constant thereafter. Differentiation marker genes (*Muc2*, *ChgA* and *CA2*) were expressed over 60 d. The primers used are listed in **Supplementary Table 1**. (**b**) RT-PCR shows that *Lgr5* upregulation is mediated by a combination of minimum factors (Wnt3a, Rspo1 and BSA) and Noggin but not by EGF and HGF. (**c**) Notch signal-mediated cell fate determination *in vitro*. Cultured organoids were treated with GSI, LY-411575 or vehicle alone from day 4 to day 8. Organoids stained with alcian blue are shown (left). Scale bar, 50 μm. RT-PCR shows that the expression of *Muc2* is upregulated, whereas the expression of *Lgr5* is reciprocally downregulated in organoids treated with LY-411575 (GSI, right). Similar results were obtained in three independent experiments, and representative data are shown. (**d**) A time-lapse imaging of a growing colonic crypt obtained from an *Lgr5-EGFP-ires-CreERT2* mouse over 192 h. The top panel shows EGFP and the bottom panel shows merged images of EGFP and differential interference contrast (DIC). Scale bar, 50 μm. The corresponding video (**Supplementary Video 3**) and similar results from another example are available as **Supplementary Figure 4a** and **Supplementary Video 4**.

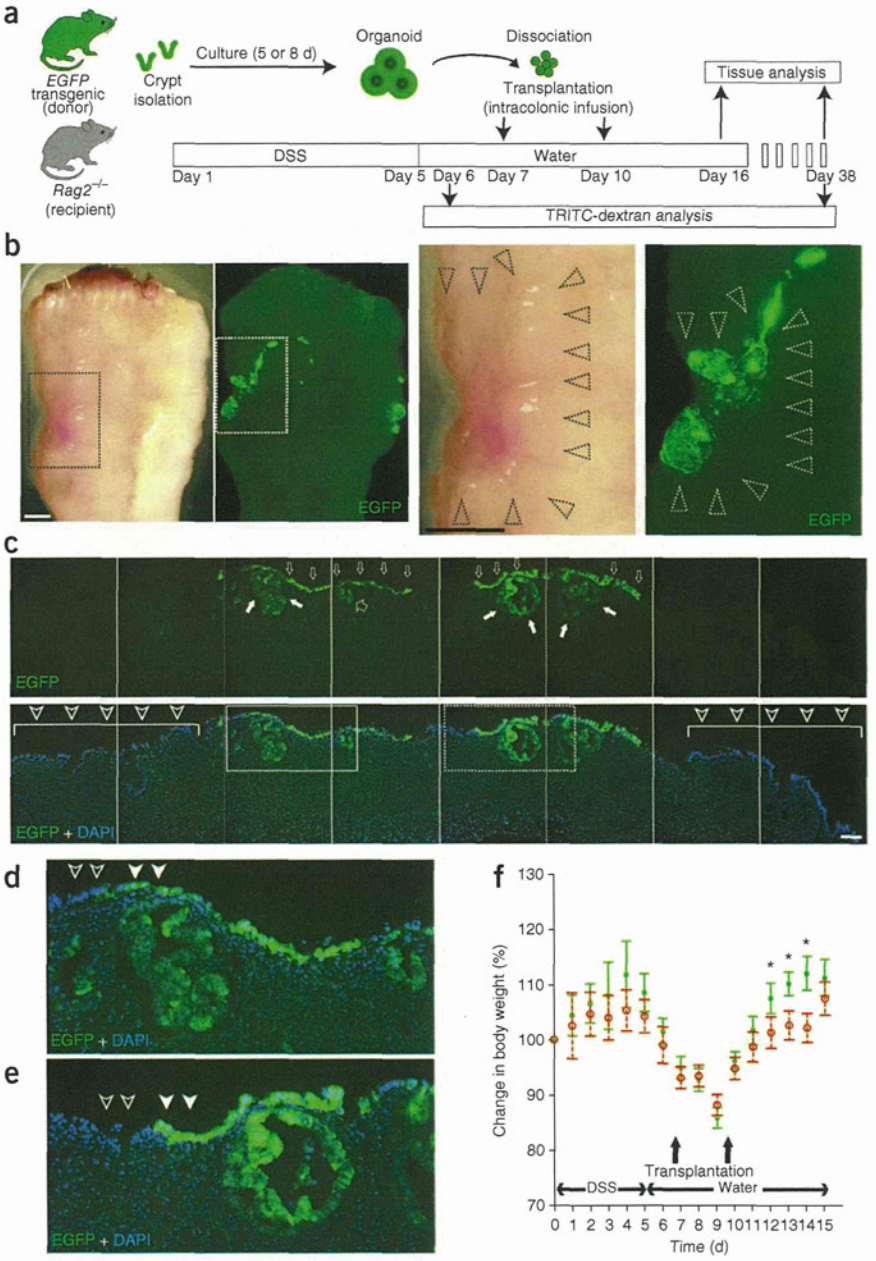

Figure 3 Transplantation of cultured cells improves acute colitis. (**a**) Experimental protocols. (**b**) Recipient colon at 6 d after transplantation. Low-power views (stereoscopic and fluorescent images) are shown on the left. High-power views of the areas in the dotted squares are shown in the right. The black dotted arrowheads show a depressed area surrounded by edematous mucosa. EGFP$^+$ areas overlapping the damaged region (white dotted arrowheads) are also shown. Note that the outline of the tissue is not precisely the same in the stereoscopic and fluorescent images, as they were acquired on different microscopes. Scale bars, 1 mm. (**c**) Histology of the EGFP$^+$ area shown in **b**. EGFP (top) and the merged image with DAPI staining (bottom). EGFP$^+$ cells cover the damaged mucosa that intervene separate areas preserving crypt structures (bottom, arrowheads). EGFP$^+$ cells constitute flat linings (top, narrow open arrow) or an invagination (top, wide open arrows), the latter of which is reminiscent of crypts. EGFP$^+$ cystic structures were also observed in the EGFP$^+$ cells (top, filled white arrows). The regions in the solid- and dotted-line boxes are shown at higher magnification in **d** and **e**, respectively. Scale bar, 100 μm. (**d**) High-power view of the solid box in **c**. (**e**) High-power view of the dotted box in **c**. (**f**) *Rag2*$^{-/-}$ mice were given DSS for 5 d, and then transplantation ($n = 6$) or sham-transplantion ($n = 6$) was performed. On day 16, the presence of engraftment was retrospectively assessed after the mice were killed. The body weights of the mice with EGFP$^+$ engraftment (green squares, $n = 4$) and sham-transplanted controls (red open circles, $n = 6$) are presented as a percentage of their initial weight. Error bars, s.e.m. $^*P < 0.05$ (Student's t test).

differentiation of progenitors[23,24] and stem cells[25] toward secretory lineages. We treated the colonic organoids with LY-411575, a γ-secretase inhibitor (GSI) that is capable of inhibiting Notch signaling[26,27]. Notch inhibition induced a goblet-cell phenotype with an increased level of *Muc2* mRNA and a reciprocal decrease in the expression of *Lgr5* (**Fig. 2c**).

We next performed live imaging of colonic organoids obtained from *Lgr5-EGFP-internal ribosome entry site (ires)-CreERT2* mice[6] in which an enhanced GFP (EGFP) and tamoxifen-inducible Cre recombinase cassette is integrated into the *Lgr5* locus. The *Lgr5*-promoter–driven EGFP expression initially stayed at a marginal level but then increased beginning at day 5 (**Fig. 2d**, **Supplementary Fig. 4a** and **Supplementary Videos 3** and **4**). We confirmed the expansion of Lgr5$^+$ cells at a single-cell resolution (**Supplementary Fig. 4b**). Over multiple passages, the *Lgr5-EGFP* locus tended to become silenced, whereas the wild-type *Lgr5* allele remained active (**Fig. 2a**,**b**). Taken together, colonic Lgr5$^+$ stem cells were able to self renew and expand *in vitro*.

Cultured colonic organoids rescue damaged epithelium

We next tested the transplantability of the cultured organoids (**Fig. 3a**). We induced colonic mucosal damage by providing immunocompromised *Rag2*$^{-/-}$ mice with colitis-inducing dextran sulfate sodium (DSS)[28] for 5 d. Most of the mice developed acute colitis characterized by weight loss, bloody stool, diarrhea and epithelial injury in the distal colon. At 7 and 10 d after initiating DSS administration, we dissociated the organoids cultured from *EGFP* transgenic mice[29] into small fragments, suspended them in a Matrigel-containing PBS and instilled them by enema in recipient mice.

At 16 d after the start of DSS administration, the recipient colons showed varying degrees of recovery. Multiple EGFP$^+$ areas appeared as well-demarcated patches in the treated colons (**Fig. 3b**). We did not observe any EGFP$^+$ areas in colons not treated with DSS (data not shown). Histologically, the EGFP$^+$ cells covered the submucosa and were located between the less damaged recipient tissues (**Fig. 3c**). The EGFP$^+$ cells formed flat or slightly invaginated linings (**Fig. 3c**). We also observed large cystic EGFP$^+$ structures below the surface of the treated colons (**Fig. 3c**). Some of the EGFP$^+$ areas connected to the recipients' epithelium (**Fig. 3d**), whereas others repopulated areas that were devoid of recipient epithelium (**Fig. 3e**). Notably, the body weights of the mice with engraftment were

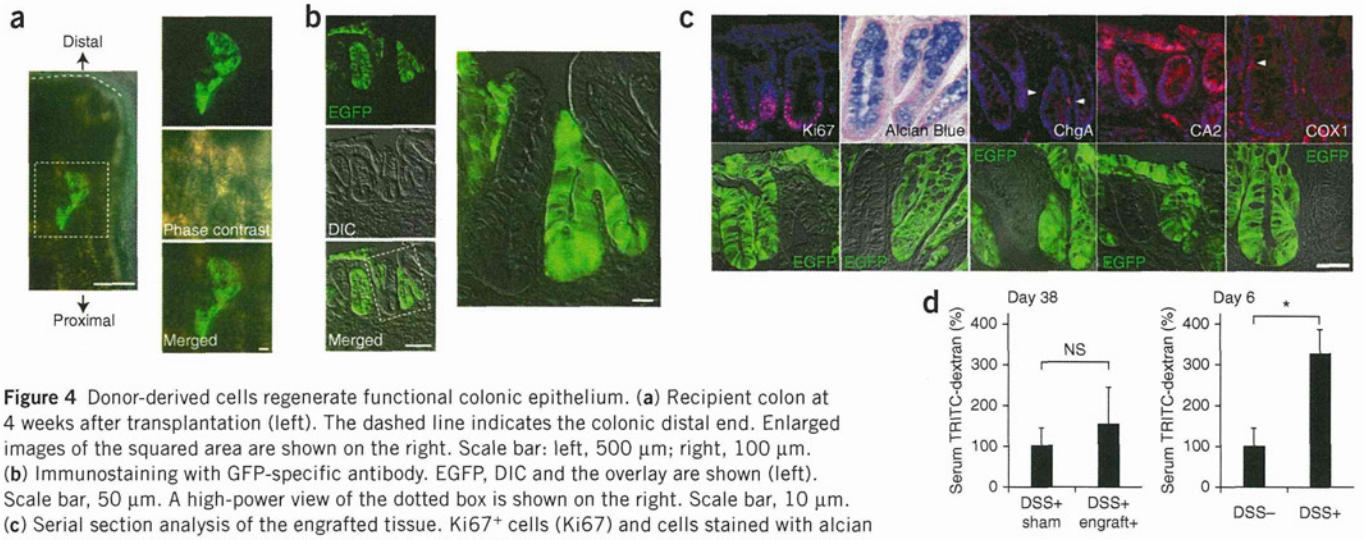

Figure 4 Donor-derived cells regenerate functional colonic epithelium. (**a**) Recipient colon at 4 weeks after transplantation (left). The dashed line indicates the colonic distal end. Enlarged images of the squared area are shown on the right. Scale bar: left, 500 μm; right, 100 μm. (**b**) Immunostaining with GFP-specific antibody. EGFP, DIC and the overlay are shown (left). Scale bar, 50 μm. A high-power view of the dotted box is shown on the right. Scale bar, 10 μm. (**c**) Serial section analysis of the engrafted tissue. Ki67$^+$ cells (Ki67) and cells stained with alcian blue (goblet cells) or immunostained for ChgA, CA2 and COX1 are shown. Images are shown with or without DAPI staining. The bottom row shows neighboring sections stained for GFP. Arrowheads point to ChgA$^+$ or COX1$^+$ cells. Scale bar, 50 μm. (**d**) After DSS colitis induction, transplantation ($n = 6$) or sham transplantation ($n = 6$) was performed. Mice were administered TRITC-dextran by gavage before killing on day 38. Four out of six colons in the transplanted group had EGFP$^+$ engraftment, and the serum TRITC concentration in these mice is shown (DSS+ engraft+; $n = 4$) as a percentage of that in the sham-transplanted group (DSS+ sham; $n = 6$). As a control, DSS colitis was induced (DSS+; $n = 6$) or uninduced (DSS–; $n = 6$) in *Rag2*$^{-/-}$ mice, and these mice were subjected for the same assay on day 6 without transplantation. Data are shown as a percentage of the concentrations in uninduced mice. Error bars, s.e.m. $^*P < 0.05$, NS, not significant (Student's *t* test).

higher than those of sham-transplanted mice (**Fig. 3f**; with statistically significant results at days 12, 13 and 14, $P < 0.05$).

At 4 weeks after transplantation, tube-like EGFP$^+$ crypts appeared in the distal colon (**Fig. 4a**) that were morphologically indistinguishable from the surrounding EGFP$^-$ epithelium (**Fig. 4b**). Notably, the engrafted crypts were entirely EGFP$^+$, indicating the presence of EGFP$^+$ stem cells (**Fig. 4b**). Cells in the lower part of the EGFP$^+$ crypts were normally Ki67$^+$, and the EGFP$^+$ crypts contained all

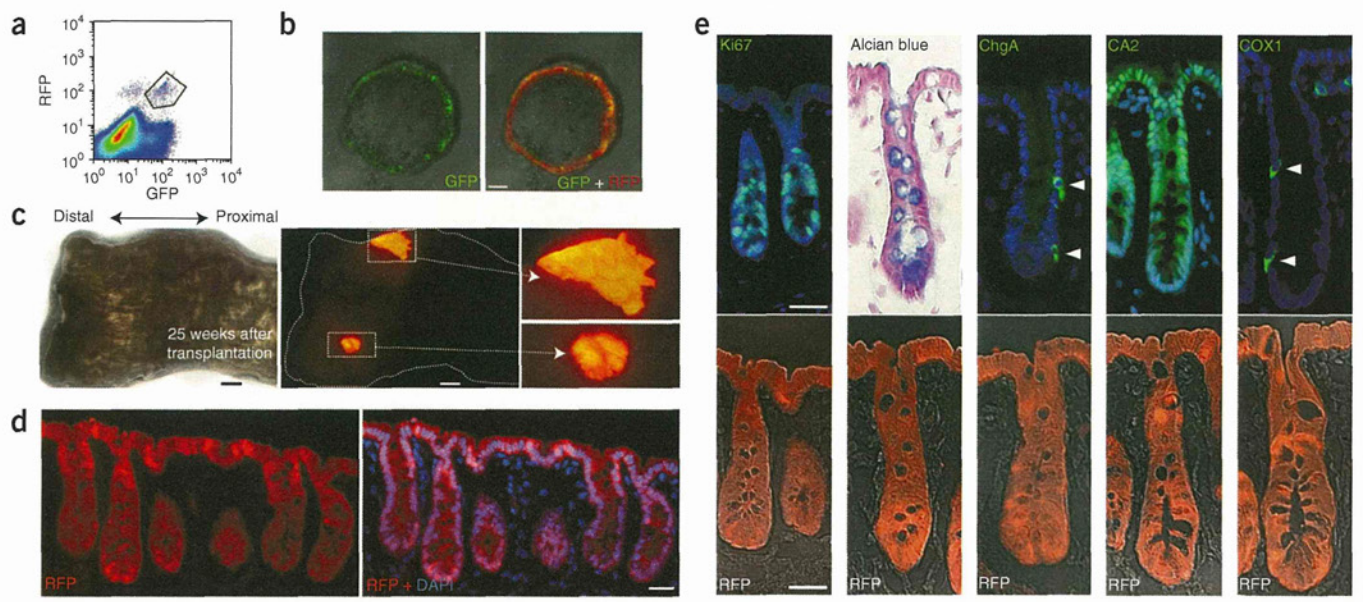

Figure 5 Single Lgr5$^+$ stem-cell–derived cultured cells serve as long-lived, multipotential stem cells *in vivo*. (**a**) Fluorescence-activated cell sorting analysis of colonic cells of *R26R-Confetti* mice crossed with *Lgr5-EGFP-ires-CreERT2* mice 3 d after Cre induction. The EGFP$^+$ and RFP$^+$ populations located in the box were sorted and cultured. (**b**) Images are shown of one out of four organoids grown from sorted single Lgr5$^+$ cells at day 6. EGFP$^+$ stem cells are scattered in the organoid (left), with all the offspring being positive for RFP (right). Scale bar, 50 μm. (**c**) Images of the recipient colon at 25 weeks after transplantation. The phase-contrast view of the recipient colon is shown on the left. The fluorescent image shows the tissue contains RFP$^+$ grafts (right). Scale bar, 1 mm. Enlarged images of the boxed areas are also shown (2.7-fold magnification). (**d**) Immunostaining of the RFP$^+$ engraft at 25 weeks after transplantation. An image of RFP-specific antibody staining (left) and an image of RFP staining merged with DAPI staining (right) are shown. Scale bar, 50 μm. (**e**) Serial section analysis of the engrafted RFP$^+$ tissue at 25 weeks after transplantation. The top panels show Ki67, alcian blue, ChgA, CA2 or COX1 staining with or without nuclei stained by DAPI. The bottom panels show the adjacent sections stained for RFP. Arrowheads point to ChgA$^+$ enteroendocrine cells and COX1$^+$ tuft cells. Scale bars, 50 μm.

terminally differentiated cell types (**Fig. 4c**). We probed the epithelial permeability of the engrafts using tetramethylrhodamine isothiocyanate (TRITC)-conjugated dextran (TRITC-dextran). Blood TRITC concentrations in transplanted mice were comparable to those in control mice, indicating a maintenance of epithelial barrier function in these engrafts (**Fig. 4d**). Notably, transplantation was less successful with freshly isolated donor cells ($P < 0.05$, Mann-Whitney U test; **Supplementary Fig. 5**), suggesting that the expansion of stem cells during the culture is associated with a higher success rate of transplantation. In addition, Matrigel-containing organoid suspensions transplanted better than organoids suspended in PBS (**Supplementary Fig. 5**; $P < 0.05$, Mann-Whitney U test), proposing a role for the simultaneous supply of extracellular matrix in successful transplantation.

Engraftment of organoids derived from a single Lgr5$^+$ cell

We next sought to initiate the protocol described above from a single stem cell (**Supplementary Fig. 6a**). We crossed *Lgr5-EGFP-ires-CreERT2* mice with *R26R-Confetti* reporter mice[30]. In the resulting offspring, tamoxifen-induced Cre activation resulted in Cre-mediated recombination at the *Rosa26* locus in individual Lgr5$^+$ stem cells, leading to stochastically selected expression of one out of four fluorescent proteins: red fluorescent protein (RFP), cyan fluorescent protein (CFP), GFP or yellow fluorescent protein (YFP). At 3 d after Cre activation, we sorted cells double positive for Lgr5-EGFP and Confetti-RFP, which consisted of ~0.02% of the total cells (**Fig. 5a**), equivalent to ~100 cells per mouse.

We cultured the sorted cells after a limiting dilution (100 cells per 96 well) using the Hubrecht protocol (Online Methods; protocol described previously[12] with addition of Y-27632 in the first 2 d). Four stem cells double positive for Lgr5-EGFP and Confetti-RFP grew out, which was comparable to the culture efficiency of small intestinal stem cells[11] (**Fig. 5b**). Organoids were expanded to more than 100 wells in >10 weeks, frozen and shipped. After thawing, we recovered the cells under the TMDU protocol. We transplanted ~500 organoids per recipient mouse, as described above. Analyses at 4, 17, 21 and 25 weeks after transplantation revealed the presence of grafts in these mice (**Fig. 5c** and **Supplementary Figs. 6b,c** and **7a**). At 25 weeks after transplantation, RFP$^+$ cells still generated a single-layered epithelium. We noted no sign of adenomatous or dysplastic change in any of the transplanted areas (**Fig. 5d**). Again, all differentiated cell types, as well as Ki67$^+$ proliferating cells, were present at normal ratios (**Fig. 5e** and **Supplementary Fig. 7b**).

DISCUSSION

Here we describe methodologies to isolate, culture and transplant Lgr5$^+$ colon stem cells. Our observations confirm that *Lgr5* marks genuine stem cells that retain their self-renewal and multilineage-differentiation properties even after prolonged culture. A major difference between small-intestinal and colon-culture conditions is in the latter's requirement for Wnt. Although Wnt factors can initiate Wnt signals on their own, R-spondins (such as Rspo1) can only augment preexisting Wnt signals[31]. Because Paneth cells produce Wnt3, they serve as the center of organization of the stem cell niche[19]. At the colon crypt bottoms, secretory cells are located between the Lgr5$^+$ stem cells that—like Paneth cells—express CD24 (ref. 19). However, these CD24$^+$ secretory cells do not produce a sufficient amount of Wnt proteins *in vitro* (data not shown). Therefore, colon organoids cannot grow from Rspo1 alone but, rather, also require exogenous Wnt.

This study provides proof of principle that cultured Lgr5$^+$ cells can be used for stem-cell therapy to repair damaged epithelium. Transplanted cells adhere to and cover superficially damaged tissue. Further, engrafted recipient mice had higher body weights than ungrafted controls, implying a beneficial role for the donor cells in DSS-induced acute colitis. Although further optimization is clearly needed, the current study implies that *in vitro* expansion and transplantation of gastrointestinal stem cells may be a promising option for patients with severe gastrointestinal epithelial injuries.

Lgr5$^+$ stem cells divide once every day *in vivo*[6], thus defying the Hayflick limit[32]. They appear similarly unrestricted in their proliferative capacity *in vitro*, while they retain their original tissue identity. It is of interest that the Lgr5 protein is now known to reside in the Wnt receptor complex to function as a receptor for Rspo1 (refs. 33,34), which is a crucial component of long-term organoid culture systems that we have developed. As the resulting organoids have now been proven to be transplantable, the Lgr5$^+$ stem cell isolation and expansion technology may provide a simple and safe avenue for the development of new regenerative and gene-therapy strategies.

METHODS

Methods and any associated references are available in the online version of the paper at http://www.nature.com/naturemedicine/.

Note: Supplementary information is available on the Nature Medicine website.

ACKNOWLEDGMENTS

We thank M. Okabe (Osaka University) for EGFP transgenic mice and Y. Kato, J. Inazawa, I. Sekiya (TMDU), H. Snippert and R. Vries (Hubrecht Institute) for technical assistance. This study was supported by Grant-in-Aid for Scientific Research from the Japanese Ministry of Education, Culture, Sports, Science and Technology, by the Health and Labour Sciences Research Grants for Research on Intractable Diseases from Ministry of Health, Labour and Welfare of Japan, and by a grant from the European Research Council and from the Dutch Cancer Foundation.

AUTHOR CONTRIBUTIONS

T. Nakamura, H.C. and M.W. designed the study. S.Y., T. Nakamura and T.S. performed experiments and analyzed data. T. Nakamura, T.S. and H.C. wrote the paper. Y.N., T. Nagaishi and K.T. assisted in transplantation experiments. T.M., X.Z. and K.T. gave support in gene analysis. R.O. helped with the immunohistochemistry. S.I. advised on the electron microscopy. H.C. and M.W. gave conceptual advice and supervised the project.

COMPETING FINANCIAL INTERESTS

The authors declare competing financial interests: details accompany the full-text HTML version of the paper at http://www.nature.com/naturemedicine/.

Published online at http://www.nature.com/naturemedicine/.
Reprints and permissions information is available online at http://www.nature.com/reprints/index.html.

1. Potten, C.S., Booth, C. & Pritchard, D.M. The intestinal epithelial stem cell: the mucosal governor. *Int. J. Exp. Pathol.* **78**, 219–243 (1997).
2. Bjerknes, M. & Cheng, H. Intestinal epithelial stem cells and progenitors. *Methods Enzymol.* **419**, 337–383 (2006).
3. Barker, N., van de Wetering, M. & Clevers, H. The intestinal stem cell. *Genes Dev.* **22**, 1856–1864 (2008).
4. Crosnier, C., Stamataki, D. & Lewis, J. Organizing cell renewal in the intestine: stem cells, signals and combinatorial control. *Nat. Rev. Genet.* **7**, 349–359 (2006).
5. Radtke, F. & Clevers, H. Self-renewal and cancer of the gut: two sides of a coin. *Science* **307**, 1904–1909 (2005).
6. Barker, N. *et al.* Identification of stem cells in small intestine and colon by marker gene *Lgr5*. *Nature* **449**, 1003–1007 (2007).
7. Barker, N. *et al.* Lgr5^{+ve} stem cells drive self-renewal in the stomach and build long-lived gastric units *in vitro*. *Cell Stem Cell* **6**, 25–36 (2010).
8. Sangiorgi, E. & Capecchi, M.R. *Bmi1* is expressed *in vivo* in intestinal stem cells. *Nat. Genet.* **40**, 915–920 (2008).
9. Avansino, J.R., Chen, D.C., Woolman, J.D., Hoagland, V.D. & Stelzner, M. Engraftment of mucosal stem cells into murine jejunum is dependent on optimal dose of cells. *J. Surg. Res.* **132**, 74–79 (2006).
10. Tait, I.S., Evans, G.S., Flint, N. & Campbell, F.C. Colonic mucosal replacement by syngeneic small intestinal stem cell transplantation. *Am. J. Surg.* **167**, 67–72 (1994).

11. Sato, T. *et al.* Single Lgr5 stem cells build crypt-villus structures *in vitro* without a mesenchymal niche. *Nature* **459**, 262–265 (2009).
12. Sato, T. *et al.* Long-term expansion of epithelial organoids from human colon, adenoma, adenocarcinoma, and Barrett's epithelium. *Gastroenterology* **141**, 1762–1772 (2011).
13. Booth, C., Patel, S., Bennion, G.R. & Potten, C.S. The isolation and culture of adult mouse colonic epithelium. *Epithelial Cell Biol.* **4**, 76–86 (1995).
14. Whitehead, R.H., Demmler, K., Rockman, S.P. & Watson, N.K. Clonogenic growth of epithelial cells from normal colonic mucosa from both mice and humans. *Gastroenterology* **117**, 858–865 (1999).
15. Kanayama, M. *et al.* Hepatocyte growth factor promotes colonic epithelial regeneration via Akt signaling. *Am. J. Physiol. Gastrointest. Liver Physiol.* **293**, G230–G239 (2007).
16. Tahara, Y. *et al.* Hepatocyte growth factor facilitates colonic mucosal repair in experimental ulcerative colitis in rats. *J. Pharmacol. Exp. Ther.* **307**, 146–151 (2003).
17. Kim, K.A. *et al.* Mitogenic influence of human R-spondin1 on the intestinal epithelium. *Science* **309**, 1256–1259 (2005).
18. Wei, Q. *et al.* R-spondin1 is a high affinity ligand for LRP6 and induces LRP6 phosphorylation and β-catenin signaling. *J. Biol. Chem.* **282**, 15903–15911 (2007).
19. Sato, T. *et al.* Paneth cells constitute the niche for Lgr5 stem cells in intestinal crypts. *Nature* **469**, 415–418 (2011).
20. Gerbe, F. *et al.* Distinct ATOH1 and Neurog3 requirements define tuft cells as a new secretory cell type in the intestinal epithelium. *J. Cell Biol.* **192**, 767–780 (2011).
21. Watanabe, K. *et al.* A ROCK inhibitor permits survival of dissociated human embryonic stem cells. *Nat. Biotechnol.* **25**, 681–686 (2007).
22. Haramis, A.P. *et al. De novo* crypt formation and juvenile polyposis on BMP inhibition in mouse intestine. *Science* **303**, 1684–1686 (2004).
23. Fre, S. *et al.* Notch signals control the fate of immature progenitor cells in the intestine. *Nature* **435**, 964–968 (2005).
24. van Es, J.H. *et al.* Notch/γ-secretase inhibition turns proliferative cells in intestinal crypts and adenomas into goblet cells. *Nature* **435**, 959–963 (2005).
25. van Es, J.H., de Geest, N., van de Born, M., Clevers, H. & Hassan, B.A. Intestinal stem cells lacking the Math1 tumour suppressor are refractory to Notch inhibitors. *Nat. Commun.* **1**, 18 (2010).
26. Wong, G.T. *et al.* Chronic treatment with the γ-secretase inhibitor LY-411,575 inhibits β-amyloid peptide production and alters lymphopoiesis and intestinal cell differentiation. *J. Biol. Chem.* **279**, 12876–12882 (2004).
27. Okamoto, R. *et al.* Requirement of Notch activation during regeneration of the intestinal epithelia. *Am. J. Physiol. Gastrointest. Liver Physiol.* **296**, G23–G35 (2009).
28. Wirtz, S., Neufert, C., Weigmann, B. & Neurath, M.F. Chemically induced mouse models of intestinal inflammation. *Nat. Protoc.* **2**, 541–546 (2007).
29. Okabe, M., Ikawa, M., Kominami, K., Nakanishi, T. & Nishimune, Y. 'Green mice' as a source of ubiquitous green cells. *FEBS Lett.* **407**, 313–319 (1997).
30. Snippert, H.J. *et al.* Intestinal crypt homeostasis results from neutral competition between symmetrically dividing Lgr5 stem cells. *Cell* **143**, 134–144 (2010).
31. Binnerts, M.E. *et al.* R-Spondin1 regulates Wnt signaling by inhibiting internalization of LRP6. *Proc. Natl. Acad. Sci. USA* **104**, 14700–14705 (2007).
32. Hayflick, L. & Moorhead, P.S. The serial cultivation of human diploid cell strains. *Exp. Cell Res.* **25**, 585–621 (1961).
33. de Lau, W. *et al.* Lgr5 homologues associate with Wnt receptors and mediate R-spondin signalling. *Nature* **476**, 293–297 (2011).
34. Carmon, K.S., Gong, X., Lin, Q., Thomas, A. & Liu, Q. R-spondins function as ligands of the orphan receptors LGR4 and LGR5 to regulate Wnt/β-catenin signaling. *Proc. Natl. Acad. Sci. USA* **108**, 11452–11457 (2011).

ONLINE METHODS

Mice. *Rag2*$^{-/-}$ mice were from Taconic Farms and Central Laboratories for Experimental Animals. *EGFP* transgenic mice[29], *Lgr5-EGFP-ires-CreERT2* mice[6] and *R26R-Confetti* mice[30] are described elsewhere. Male and female mice were randomly used for all experiments. All animal experiments were performed with the approval of the Institutional Animal Care and Use Committee of TMDU.

TMDU protocol for crypt isolation and three-dimensional culture. The colonic tissue was minced and digested. The crypts were further purified by mechanical disruption and density gradient centrifugation. A total of 2,000 crypts were suspended in 200 µl of the collagen type I solution (Nitta Gelatin Inc.) and placed in 48-well plates. After polymerization, 500 µl of Advanced DMEM/F12 containing BSA (Sigma), mouse EGF (mEGF) (PeproTech), mWnt3a, mRspo1, mHGF and mNoggin (all from R&D Systems) was added (TMDU medium). For passage, the gel was digested, and then the organoids were disaggregated with EDTA. The dissociated organoids were mixed in type I collagen solution and used for culture. A Rho kinase inhibitor, Y-27632, was added for the first 2 d after the cells were propagated. Where indicated, to induce goblet cell differentiation, organoids were treated with LY-411575, a GSI. See details in the **Supplementary Methods**.

Chromosome analysis. Chromosome karyotyping was performed according to a standard protocol as detailed in the **Supplementary Methods**.

Stereomicroscopy, phase-contrast imaging and histology. Images were acquired on either a fluorescence microscope equipped with phase-contrast setting (BZ-8000, KEYENCE), a fluorescent stereomicroscope system MVX10 (Olympus) or a fluorescence microscope DeltaVision system (Applied Precision). For histology and immunohistochemistry, tissues and organoids were fixed, sequentially dehydrated in sucrose in PBS, and frozen in OCT compound (Tissue Tek). Cryosections were examined by conventional H&E, alcian blue staining and a spectrum of immunohistochemical reactions, as detailed in the **Supplementary Methods**.

Transmission electron microscopy. Transmission electron microscopy was performed in a standard fashion and is detailed in the **Supplementary Methods**.

Live imaging. Live imaging was performed on the DeltaVision system. A culture dish placed on the microscope stage was covered with a chamber in which a humidified premixed gas consisting of 5% CO_2 and 95% air was infused, and the whole setup was set at 37 °C. DIC and fluorescent images were acquired at 20-min intervals. The data were processed using Softworx (Applied Precision) and, if necessary, image editing was performed using Adobe Photoshop Elements 7.0.

Semi-quantitative RT-PCR. Semi-quantitative RT-PCR was performed in standard fashion. The primer sequences used are listed in **Supplementary Table 1**. PCR products were separated on agarose gels and visualized using ImageQuant TL system (GE Healthcare).

Sorting and Hubrecht-protocol culture for single Lgr5$^+$ cells. Tamoxifen was injected into *R26R-Confetti* mice crossed with *Lgr5-EGFP-ires-CreERT2* mice, and the colonic crypts from the resulting mice were isolated 3 d later. Epithelial cells were dissociated with TrypLE express (Invitrogen) and analyzed by MoFlo (DakoCytomation). Viable single cells were gated, and then the cells doubly positive for EGFP and RFP were sorted and embedded in Matrigel (BD Bioscience) on 96-well plates. An Advanced DMEM/F12 culture medium supplemented with penicillin and streptomycin, 4-(2-hydroxyethyl)-1-piperazineethanesulfonic acid (HEPES), glutamax, N2, B27 (all from Invitrogen) and growth factors (EGF, noggin and R-spondin) was diluted 1:1 with Wnt3a-conditioned medium and used as Hubrecht medium. Y-27632 was included for the first 2 d to avoid anoikis. Growth factors were added every other day, and the entire medium was changed every 4 d. See the **Supplementary Methods** for additional details.

Transplantation experiments. For the EGFP$^+$ cell transplantations, cells isolated from colon tissues were cultured for 5 or 8 d according to the TMDU protocol and used as donor cells. For single Lgr5$^+$-cell–derived organoid transplantation, cells were expanded based on the Hubrecht protocol and then cryopreserved. The cells were then shipped, thawed and further cultured. Acute colitis was induced by feeding 6-week-old *Rag2*$^{-/-}$ mice with 3.0% DSS (molecular weight 10,000; Ensuiko Sugar Refining Co.) dissolved in drinking water for 5 d (days 1–5). At 7 and 10 d after the start of DSS administration, donor cells equivalent to those from ~500 organoids were instilled into colonic lumen as a suspension. After infusion, the anal verge was glued for 6 h. After the transplantation on day 10, mice were maintained as usual before they were killed and analyzed. See the **Supplementary Methods** for additional details.

TRITC-dextran permeability assay. Intestinal permeability was assessed by enteral administration of TRITC-dextran (molecular mass 4.4 kDa; Sigma). Transplanted or sham-transplanted mice were gavaged with TRITC-dextran 4 h before killing on day 38. Whole blood was obtained at the time of killing, and then the colonic tissues were examined for whether the EGFP$^+$ engrafts were present. TRITC-dextran measurements were performed on an ARVO MX (PerkinElmer), with serial dilutions of TRITC-dextran used as a standard curve.

Statistical analyses. Data are shown as means ± s.e.m. Data for **Figures 3f**, **4d** and **Supplementary Figure 7b** were statistically analyzed by the two-sample Student's *t* test. The data for **Supplementary Figure 5** showed non-normal distributions and were analyzed by Mann-Whitney *U* test. Statistical significance for comparisons was assigned at $P < 0.05$.

Additional methods. Detailed methodology is described in the **Supplementary Methods**.

Supplementary Information

Functional engraftment of colon epithelium expanded *in vitro* from a single adult Lgr5^{+} stem cell

Shiro Yui[1,6], Tetsuya Nakamura[2,6], Toshiro Sato[3,4], Yasuhiro Nemoto[1], Tomohiro Mizutani[1], Xiu Zheng[1], Shizuko Ichinose[5], Takashi Nagaishi[1], Ryuichi Okamoto[2], Kiichiro Tsuchiya[1], Hans Clevers[3] & Mamoru Watanabe[1]

[1] Department of Gastroenterology and Hepatology, Graduate School,
[2] Department of Advanced Therapeutics for GI Diseases,
Tokyo Medical and Dental University
1-5-45 Yushima, Bunkyo-ku, Tokyo 113-8519, Japan

[3] Hubrecht Institute and University Medical Centre Utrecht
Uppsalalaan 8, 3584 CT Utrecht, the Netherlands

[4] Current address: Department of Gastroenterology,
Keio University School of Medicine,
35 Shinanomachi, Shinjuku-ku, Tokyo 160-8582, Japan

[5] Research Center for Medical and Dental Sciences,
Tokyo Medical and Dental University
1-5-45 Yushima, Bunkyo-ku, Tokyo 113-8519, Japan

[6] These authors contributed equally

Correspondence:
H.C. (Email: h.clevers@hubrecht.eu) or M. W. (Email: mamoru.gast@tmd.ac.jp)

Contents

Supplmentary Figure 1

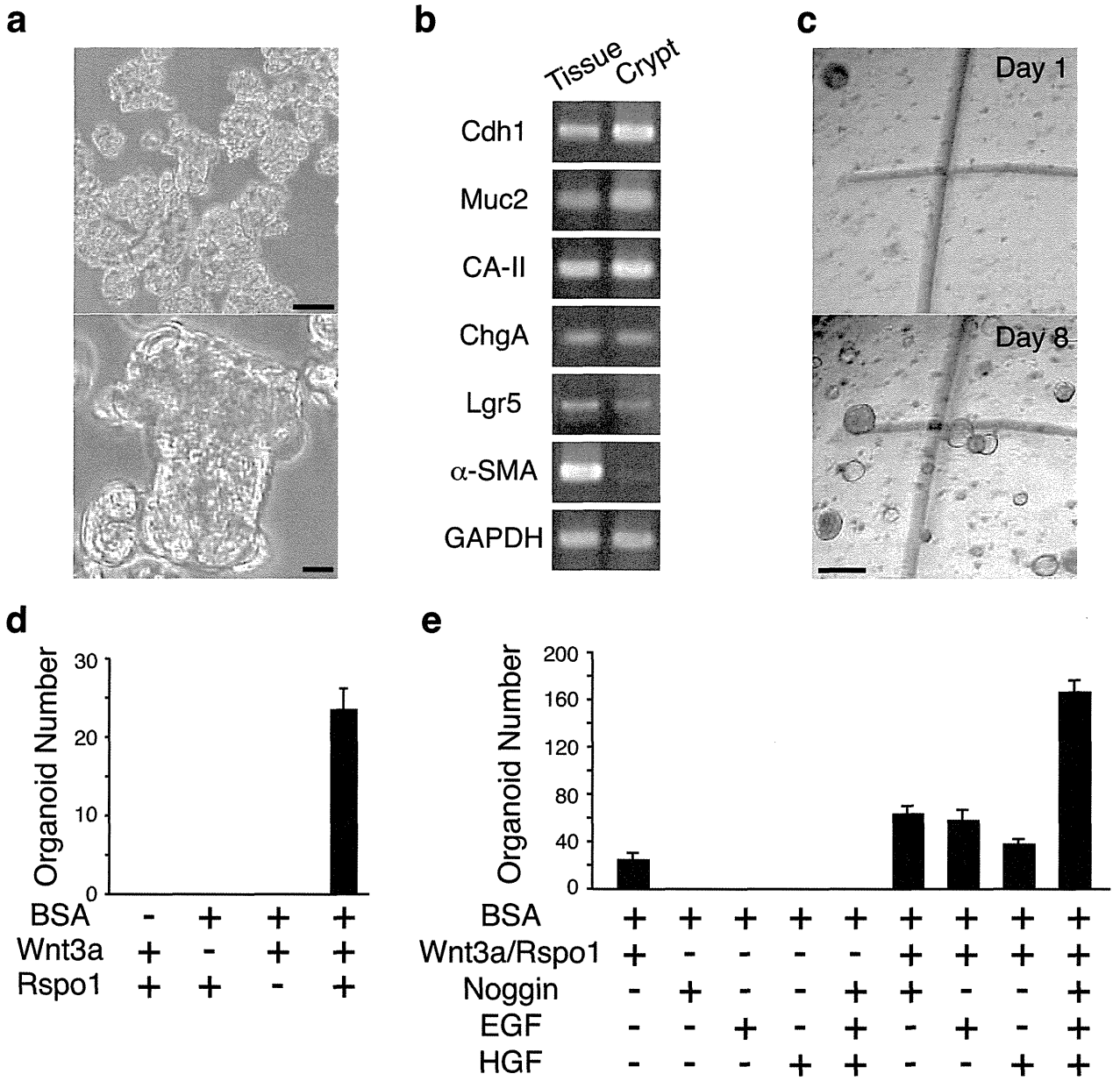

Supplementary Figure 1

Isolation and culture of colonic epithelial cells

(a) Adult mouse-derived colonic crypts isolated by collagenase, dispase, and DTT. The phase contrast views of the same field with low (top) and high (bottom) magnifications. Scale bars: top; 50 μm, bottom; 10 μm.

(b) Semi-quantitative RT-PCR shows that cells expressing epithelial genes (*Cdh1*, *Muc2*, *CA-II*, *ChgA* and *Lgr5*) are recovered while *α-SMA*$^{+}$ myofibroblasts are not. (c) Isolated crypts grow in type I collagen gel. Phase-contrast views on d 1 (top) and 8 (bottom). Marked lines serve to identify the same field in the culture dish. Scale bar, 500 μm.

(d) Effect of the factors added to the culture medium on organoid growth is shown. 2,000 crypts were seeded and cultured in the presence of indicated factors, and then organoids were counted on d 8. A combination of Wnt3a, Rspo1, and BSA was essential to maintain the colonic culture. (e) Although Noggin, EGF, or HGF was dispensable, they showed growth promoting activities. Error bars, s.e.m.; n = 3.

Supplmentary Figure 2

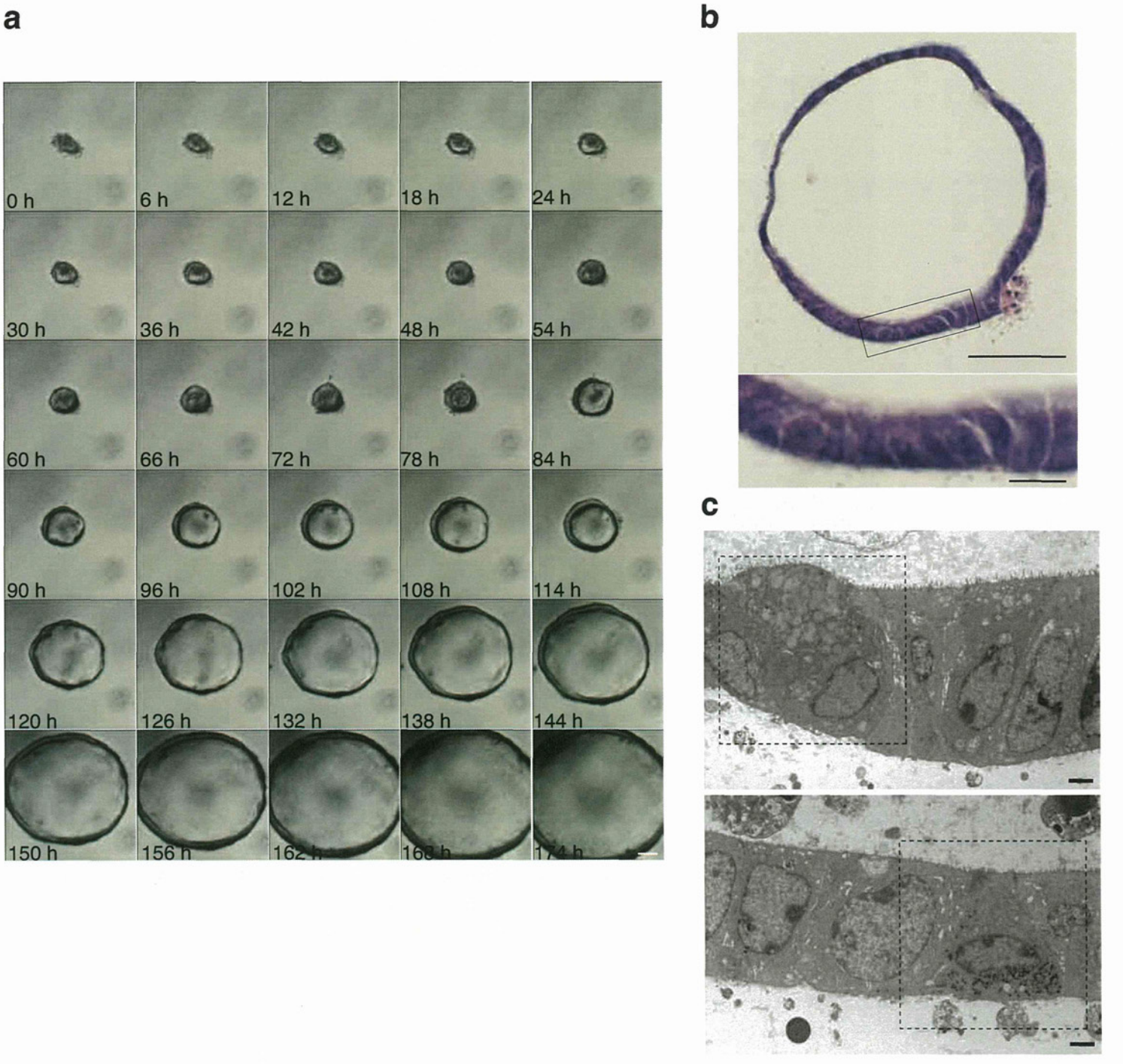

Supplementary Figure 2

Colonic crypts grow as cystic organoids consisting of single-layered epithelial cells

(a) Isolated colonic crypts were embedded in type I collagen gel and cultured in the presence of Wnt3a, Rspo1, BSA, Noggin, EGF, and HGF. Time-lapse imaging over 174 h was performed and frames from the representative video are shown. The recording started shortly after the crypt isolation, and images were acquired every 20 min. The DIC images revealed that the crypt grows rapidly, forming a round cystic structure with enclosed luminal space inside. Colonic organoids rarely exhibited budding events to form protrusion from the cystic structure. Scale bar, 50 μm. See also Supplementary Video 1. (b) Histology of the colonic organoids at d 8. H&E staining reveals that the organoids consist of single-layered cells. A higher magnification view of the top panel is shown at the bottom. Scale bars; top, 50 μm; bottom, 10 μm. (c) Transmission electron microscopy analysis at d 8 also reveals the organoids to be composed of a monolayer of cells without any non-epithelial cells underneath. Apoptotic cells are also seen in the luminal space. Scale bars, 2 μm. High magnification images in dotted squares are shown in Fig. 1f and g.

Supplmentary Figure 3

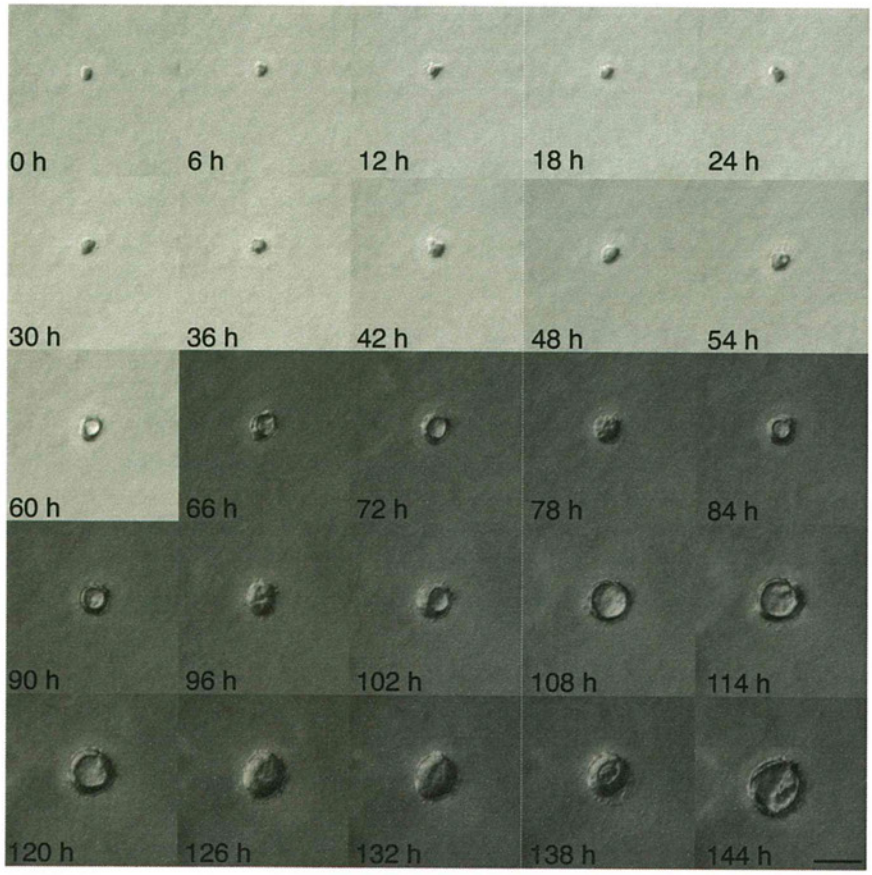

Supplementary Figure 3

Colonic organoids are built anew from single cells upon passages

Cultured colonic organoids were disaggregated and then propagated. Time-lapse imaging was performed over 144 h to track the growing organoids. Images from the representative video that shows successful organoid forming process of a single cell are shown. Scale bars, 50 μm. Corresponding video is available as Supplementary Video 2.

Supplmentary Figure 4

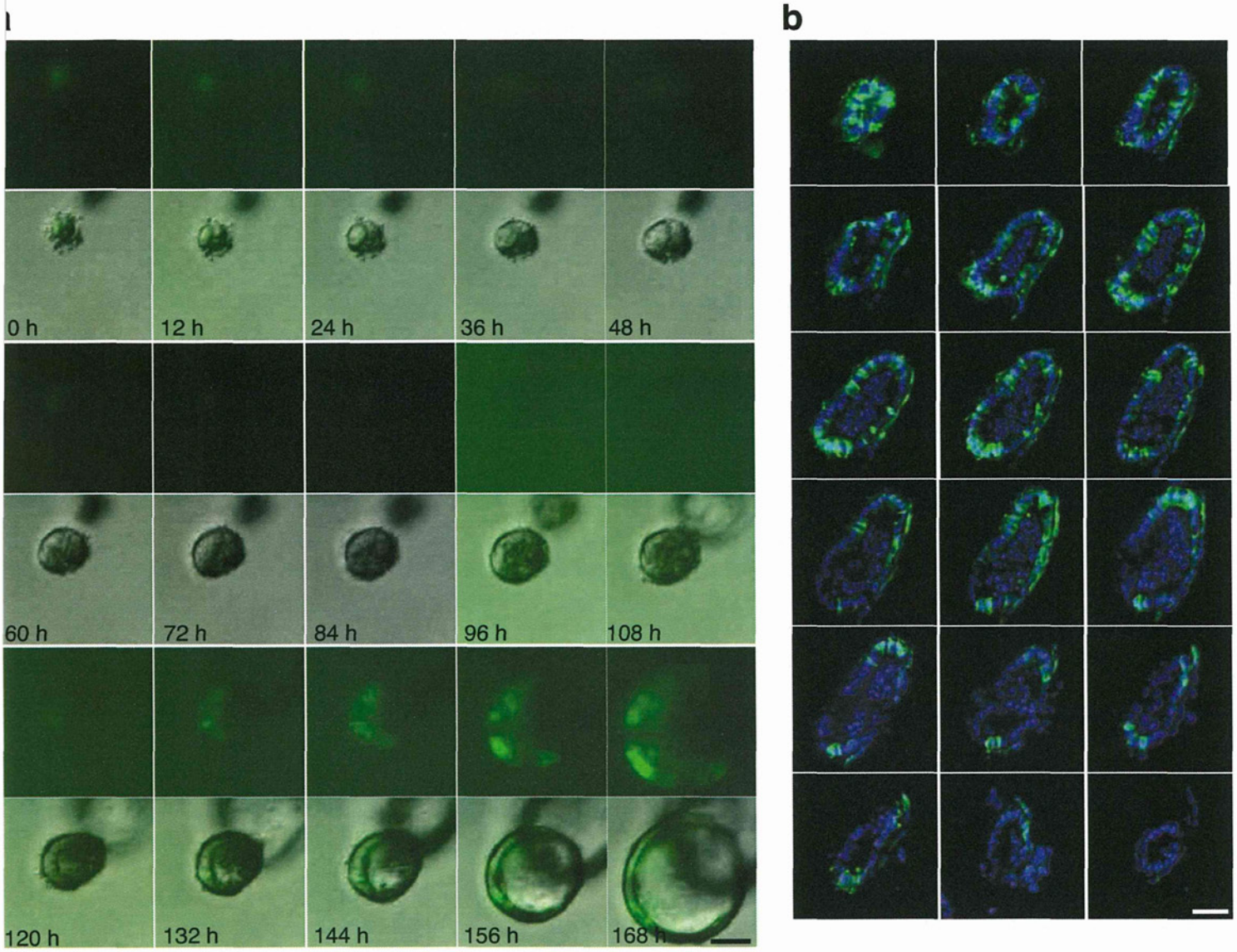

Supplementary Figure 4

Lgr5^{+} stem cells dynamically self-renew in growing organoids.

(a) This figure represents another example of the data shown in Fig. 2d. The colonic crypts were isolated from *Lgr5-EGFP-ires-CreERT2* mice and cultured. Frames from a time-lapse imaging for fluorescent and DIC images over 168 h are shown. The *Lgr5* promoter-driven EGFP expression became undetectable for the first several days, but emerged again around 120 h after starting image acquisition, and then expanded over the next few days. The top panels show EGFP fluorescence and the bottom ones show merged images of EGFP and DIC. Scale bar, 50 μm. See also Supplementary Video 4. (b) Detection of predominant expansion of Lgr5^{+} stem cells in cultured colonic organoids. Colonic crypts isolated from *Lgr5-EGFP-ires-CreERT2* mice were cultured for 6 d. Serial 6 μm thick sections of the organoids were cut and processed for imminostaining with GFP-specific antibody. Consecutive images of a representative organoid show that EGFP^{+} cells are scattered throughout the cystic structure, showing predominant proliferation of Lgr5^{+} cells in this organoid. Scale bar, 50 μm.

Supplmentary Figure 5

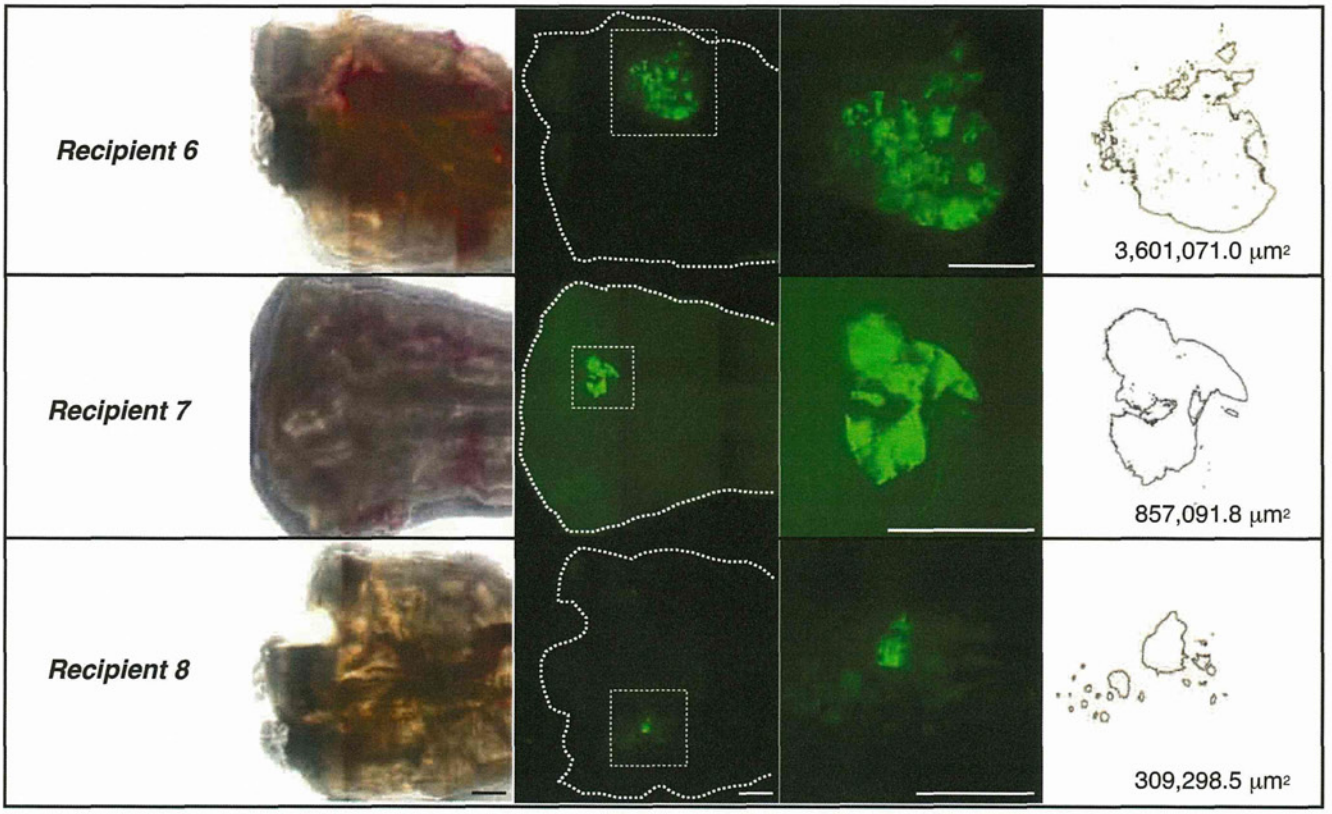

Cells Immediately After Isolation Transplanted With Matrigel		Cells From Cultured Organoids Transplanted With Matrigel		Cells From Cultured Organoids Transplanted Without Matrigel	
Recipient	Engrafted Area (μm²)	Recipient	Engrafted Area (μm²)	Recipient	Engrafted Area (μm²)
1	112,653.1	6	3,601,071.0	11	213,278.1
2	0.0	7	857,091.8	12	0.0
3	0.0	8	309,298.5	13	0.0
4	0.0	9	277,168.4	14	0.0
5	0.0	10	0.0	15	0.0
mean ±s.e.	22,530.6 ± 22,530.6	mean ±s.e.	1,008,925.9 ± 662,765.0	mean ±s.e.	42,655.6 ± 42,655.6

Supplementary Figure 5

Quantitative analysis of EGFP$^+$ engraftment

Rag2$^{-/-}$ recipient mice fed with 3% DSS for 5 d were assigned into three groups. The first group (Recipient 1 to 5) received freshly isolated EGFP$^+$ colonic cells that were suspended in a diluted Matrigel in PBS (1:20) on both d 7 and 10 after starting DSS. The second group (Recipient 6 to 10) received equivalent number of *in vitro* cultured EGFP$^+$ cells suspended in the same Matrigel/PBS solution. The third group (Recipient 11 to 15) was given the same amount of cultured EGFP$^+$ donor cells that were suspended in PBS alone. At 4 weeks after the second transplantation, the recipient tissues were analyzed. When EGFP$^+$ engraftments were present, each engrafted area was evaluated using an image software (NIH ImageJ). The typical process of the area calculation is shown (Recipient 6, 7, and 8). Phase-contrast views, EGFP images (low magnification), enlarged views for EGFP, and the area analyses are shown on the top. Scale bar, 1 mm.

Supplmentary Figure 6

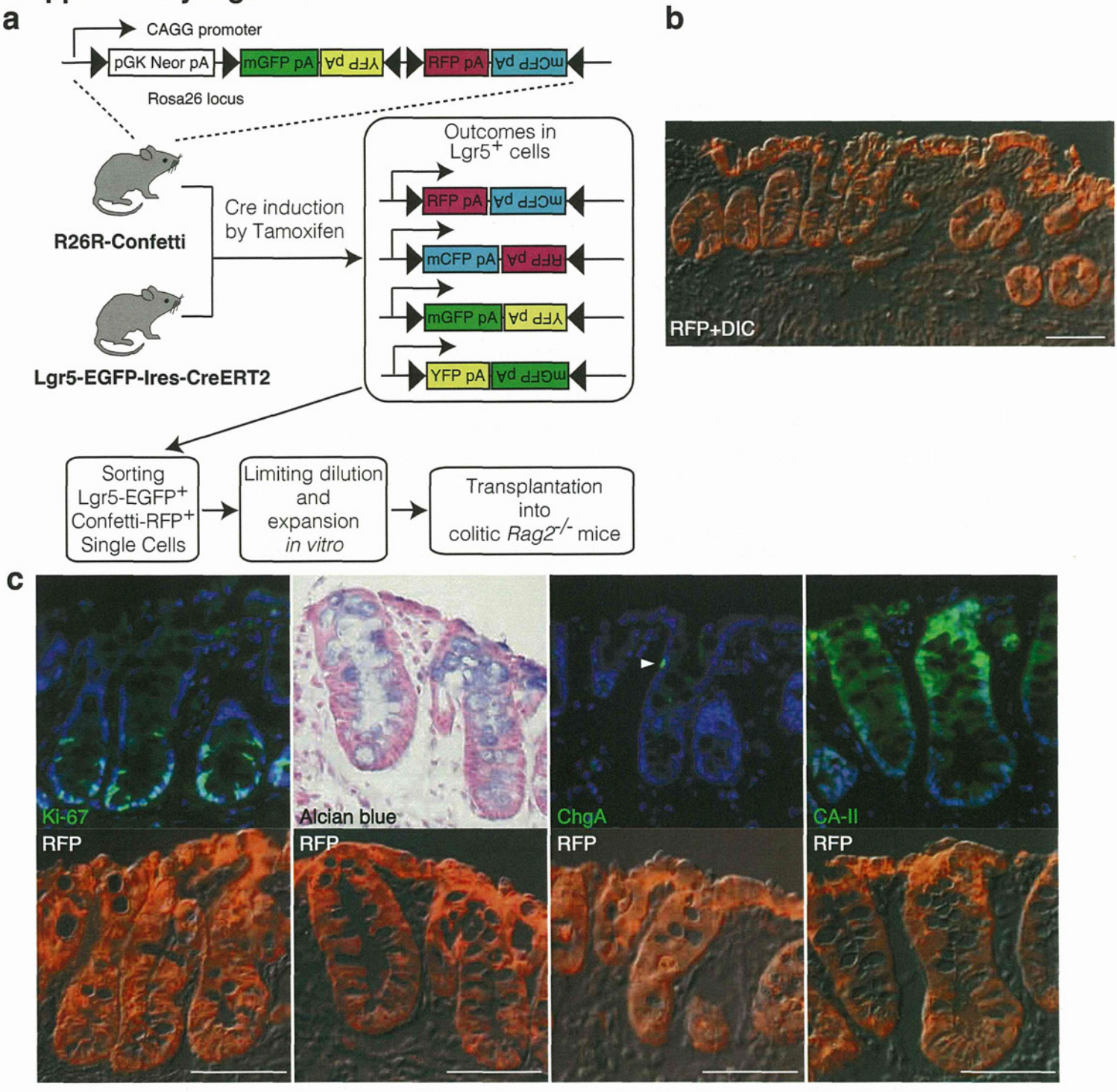

Supplementary Figure 6

Single Lgr5^{+} stem cell-derived cultured cells give rise to multiple crypts at 4 weeks post-transplantation

(a) Schematic diagram of the experiment to visualize single Lgr5^{+} cell-derived organoid expansion *in vitro* and its engraftment *in vivo*. After Cre induction in *R26R-Confetti* mice crossed with *Lgr5-EGFP-IRES-creERT2* mice, colonic crypts were isolated . Doubly positive cells for Lgr5-EGFP and Confetti-RFP were sorted and cultured. Extensively expanded RFP^{+} offsprings were transplanted into *Rag2*$^{-/-}$ recipients as described in Fig. 3. (b) Immunostaining of the grafted area with RFP-specific antibody at 4 weeks post-transplantation. An RFP image merged with DIC one is shown. A single cell-derived RFP^{+} cells constitutes multiple colonic crypts in recipients. Scale bar, 50 μm. (c) Serial sections of the engrafted tissue 4 weeks post-transplantation show the presence of Ki67^{+} proliferating cells as well as alcian blue^{+}, ChgA^{+} and CA-II^{+} differentiated cells in the crypt of donor-origin. The top panels show Ki67, alcian blue, ChgA, or CA-II staining with or without DAPI staining. The bottom panels represent the adjacent sections that were stained with RFP-specific antibody. Arrowheads point to ChgA^{+} enteroendocrine cells. Scale bar, 50 μm.

Supplmentary Figure 7

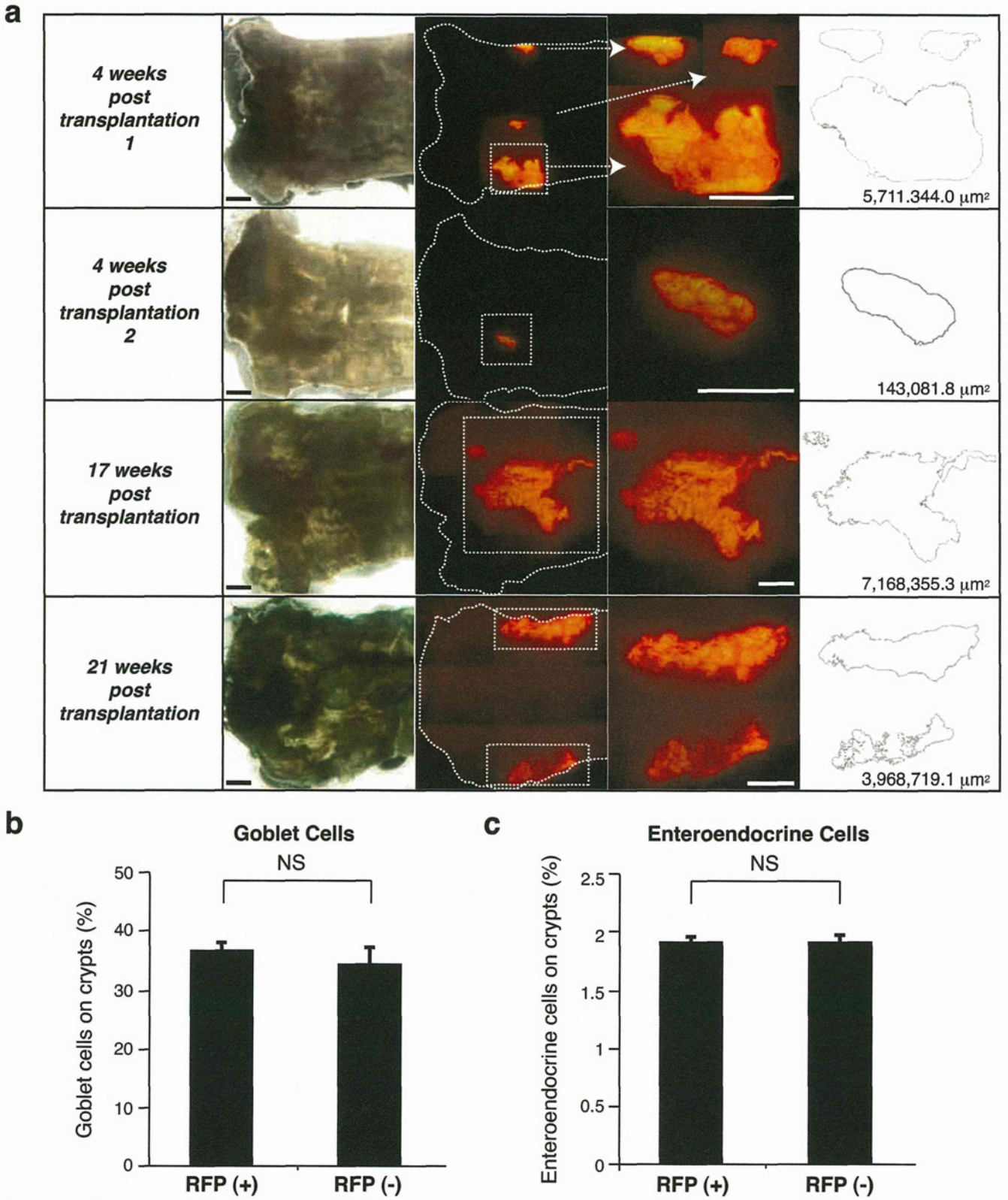

Supplementary Figure 7

Single Lgr5^{+} stem cell-derived engrafts constitute the recipients' colon over an extended time period

(a) *Rag2*$^{-/-}$ recipient mice, which were fed with DSS for 5 d and given intracolonic transplantation of single Lgr5^{+} cell-derived organoid on d 7 and 10, were sacrificed and their colons were analyzed 4 (n = 2), 17 (n = 1), 21 (n = 1), and 25 (n = 1) weeks after the second transplantation. The phase-contrast view, RFP image (low magnification), enlarged view for RFP, and the area analysis of each engraft are presented. Area calculation is done as described in Supplementary Fig. 7 by using NIH ImageJ. Scale bars, 1 mm. (b) Quantification of goblet cells were performed in RFP^{+} engraftment at 25 weeks post-transplantation. Numbers of alcian blue-positive cells were counted on both RFP^{+} engraftment and RFP^{-} recipient crypts on the same sections. Cell numbers are presented as a percentage of total epithelial cells. Error bars represent the standard error (n = 5 different sections). (c) Quantification of enteroendocrine cells, derived from counting immunostained ChgA^{+} cells was performed and shown as in (b).

Supplementary Video Legends

Supplementary Video 1
A representative colonic crypt forming a cystic structure
DIC imaging was started on the day of crypt isolation. Images were taken at 20 min intervals for a period of 174 h. Scale bar, 50 μm. See also Supplementary Figure 2a.

Supplementary Video 2
A colonic organoid grown from a single cell
A representative colonic organoid grown from a single cell after passage. DIC imaging was started on the day of propagation. Imaging interval is 20 min and the entire video represents 150 h of real time. Scale bar, 50 μm. See also Supplementary Figure 3.

Supplementary Video 3
A dynamic expansion of Lgr5^{+} stem cells in growing organoids
A growing colonic organoid obtained from *Lgr5-EGFP-ires-CreERT2* mice. The Lgr5 promoter-driven EGFP expression was visualized along with DIC imaging. Images were taken at 20 min intervals for a period of 191 h 36 min. Scale bar, 50 μm. See also Figure 2d.

Supplementary Video 4
Another example of a growing organoid showing preferential expansion of Lgr5^{+} cells
Another example of a growing organoid obtained from *Lgr5-EGFP-ires-CreERT2* mice. The imaging was performed as described in the legend for Supplementary Video 3 except for the entire time period of 168 hours. Scale bar, 50 μm. See also Supplementary Figure 4a.

Supplementary Methods

Colonic Crypt Isolation and 3D culture

Colonic crypts were isolated from adult mice at 7-9 weeks of age. The entire colon was removed and the luminal contents were flushed out with Hanks' balanced salt solution (HBSS) containing 100 U/ml penicillin, 100 μg ml^{-1} streptomycin and 50 μg ml^{-1} gentamicin. These antibiotics were added to all the solutions used for the following procedure. The tissue was repeatedly washed in HBSS, minced into small pieces, and suspended in 12.5 ml of Dulbecco's modified eagle medium (DMEM) supplemented with 1% FBS (complete DMEM) to which 500 U ml^{-1} collagenase XI (Sigma), 0.4 U ml^{-1} dispase (Roche), and 1 mM dithiothreitol (DTT) were added. The mixture was shaken for 15 min at 37°C in a water bath. To further dissociate undigested fragments, the tissues were passed through an 18-gauge needle 10 times. After 10 ml of complete DMEM was supplemented, the tube was vigorously shaken and then allowed to settle under gravity for 1 min. After the top 10 ml of the crypt suspension was transferred to a new tube, the remaining pellet was passed through the needle 5 more times, and another 10 ml of complete DMEM was added. The procedure was repeated 5 times and the liberated crypts in suspension were combined and centrifuged. The pellet was suspended in 10 ml of 30% Percoll (GE Healthcare)/HBSS and centrifuged at 860 *g* for 5 min. This density gradient centrifugation enriched the crypts since most of cellular debris, fat, and fibrous materials remained at the top of the solution. To further isolate the crypts from bacteria or single cells, the pellet was resuspended in 10 ml of complete DMEM containing 2% D-sorbitol and centrifuged at 300 *g* for 3 min. The pellet was passed through a 70-μm cell strainer (BD Bioscience) to remove large materials. The purified crypts were centrifuged, washed in Advanced DMEM/F12 (Invitrogen), and counted. After centrifugation, the final pellet of the pure crypts was used for culture.

A total of 2,000 crypts were suspended in 200 μl of the collagen type I solution (Nitta Gelatin Inc.) and placed in 48-well plates. After polymerization, 500 μl of Advanced DMEM/F12 containing 1% BSA (Sigma), 30 ng ml^{-1} mWnt3a (R&D Systems), 500 ng ml^{-1} mRspo1 (R&D Systems), 20 ng ml^{-1} mEGF (Peprotech), 50 ng ml^{-1} mHGF (R&D Systems), and 50 ng ml^{-1} mNoggin (R&D Systems) was added to each well (TMDU-medium). The medium was changed every 2 d. For passage, the whole gel was incubated in DMEM containing collagenase type XI at 37°C for 5 min. The released organoids were washed in PBS containing 0.5% BSA. The pellet was suspended in PBS containing 2 mM EDTA and 0.5% BSA, and vigorously shaken to obtain disaggregated organoids. For routine passages, the organoids were mostly dissociated into small cell clumps, mixed in type I collagen solution, and used for culture. The EDTA treatment could be extended to obtain single cells. A Rho kinase inhibitor Y-27632 was added at 10 μM for the first two days after the cells were propagated. Where indicated to induce goblet cell differentiation, organoids were treated with 100 nM of LY-411,575, a γ-secretase inhibitor, for indicated time period.

Chromosome analysis

Chromosome karyotyping was performed by an air-dry method. The cells were recovered from organoids as with the passage procedure. After centrifugation, the pellets were resuspended in 75 mM KCl solution and incubated for 15 min at 37°C. Cells were centrifuged, fixed in methanol-acetic acid (3:1), air-dried on slides, stained

with DAPI, and microscopically analyzed. A total of 10 metaphases were counted and analyzed.

Antibodies used for immunohistochemistry

The followings were used as antibodies specific for each protein: Cdh (Cell Signaling); CA-II (Santa Cruz); ChgA (for staining organoids, Santa Cruz); ChgA (for staining recipient tissue, Diasorin); Ki67 (Dako Cytomation); Cox1 (Santa Cruz); GFP (Invitrogen); DsRed (Clontech). Nuclei were counterstained with hematoxylin, DAPI, or Hoechst 33342. If necessary, image processing was carried out using Adobe Photoshop Elements 7.0 software.

Stereomicroscopy, Phase-contrast imaging and Histology

Images of the isolated crypts, growing organoids, and the whole colon tissues of recipient mice were acquired using a fluorescence microscope equipped with phase-contrast setting (BZ-8000, KEYENCE) with either PlanApo 4x 0.2NA or PlanApo 20x 0.75NA (Nikon) objectives. In some experiments, images of engrafted epithelium on damaged tissues were acquired with a fluorescent stereomicroscope system MVX10 (Olympus). Fluorescent images of sections were acquired using a DeltaVision system (Applied Precision) where a fluorescent microscope IX-71 (Olympus) with objectives UplansApo 10x 0.4NA or UplansApo 20x 0.75NA (Olympus) is incorporated. For histology and immunohistochemistry, tissues and organoids in collagen gel were fixed overnight at 4°C in 4% paraformaldehyde, sequentially dehydrated in 10, 15 and 20% sucrose in PBS, and frozen in OCT compound (Tissue Tek). Cryosections at 6-μm thickness were examined by conventional H&E staining, alcian blue staining, and a spectrum of immunohistochemical reactions as detailed previously.

Transmission Electron Microscopy

Type I collagen gel including growing organoids was fixed with 2.5% glutaraldehyde in 0.1 M PBS for 2 h, washed overnight at 4°C in the same buffer, post-fixed with 1% OsO4 buffered with 0.1 M PBS for 2 h, dehydrated in a graded series of ethanol, and embedded in Epon 812. Ultrathin (90 nm) sections were collected on copper grids, double-stained with uranyl acetate and lead citrate, and then examined with a transmission electron microscope (H-7100, Hitachi).

Live Imaging

Live imaging was performed on the DeltaVision system. A glass-bottom culture dish placed on the microscope stage was covered with a chamber in which a humidified premixed gas consisting of 5% CO_2 and 95% air was infused, and the whole setup was mounted in a temperature-controlled chamber set at 37°C. Differential interference contrast (DIC) and fluorescent images were acquired at 20 min intervals for varying time periods described in the legend for each experiment. The data were processed using softWorx (Applied Precision) and, if necessary, image editing was performed using Adbe Photoshop Elements 7.0.

Semi-quantitative RT-PCR

Total RNA was isolated using Trizol reagent (Invitrogen). 1 microgram of total RNA were used for cDNA synthesis in a 21 μl of reaction. 1 microlitter of cDNA was amplified in a 25 μl reaction. Primer sequences and the semi-quantitative conditions are shown in the Supplementary Table. PCR products were separated on agarose gels, stained by ethidium bromide, and visualized using ImageQuant TL system (GE Healthcare).

Sorting and Hubrecht-protocol Culture for Single Lgr5^{+} Cells

5 mg of tamoxifen was injected to R26R-Confetti mice crossed with *Lgr5- EGFP-IRES- creERT2* mice, and the colonic crypts were isolated 3 d after cre induction. Epithelial cells were dissociated with TrypLE express (Invitrogen) for 2 h at 37°C, passed through 20-μm cell strainer (Celltrix), washed with PBS, and analyzed by MoFlo (DakoCytomation). Viable single-cells were gated by forward scatter, side scatter, pulse-width parameter, and negative staining for propidium iodide or 7-ADD (eBioscience). Cells doubly positive for EGFP and RFP were sorted and embedded in Matrigel (BD bioscience), followed by seeding on 96-well plate. An Advanced DMEM/F12 supplemented with Penicillin/Streptomycin, 10 mM Hepes, Glutamax, 1x N2, 1x B27 (all from Invitrogen), and growth factors (50 ng ml^{-1} EGF, 100 ng ml^{-1} noggin, 1 μg ml^{-1} R-spondin) was diluted 1:1 with Wnt3a conditioned medium, and used as colonic crypt culture medium (Hubrecht medium). Y-27632 (10 μM) was included for the first 2 d to avoid anoikis. Growth factors were added every other day and the entire medium was changed every 4 d.

Transplantation experiment

For EGFP^{+} cell transplantations, cells isolated from colon tissues of *EGFP* transgenic mice were cultured for 5 or 8 d according to the TMDU-protocol and used as donor cells. For single Lgr5^{+} cell-derived organoid transplantation, sorted EGFP^{+}/RFP^{+} cells were expanded based on the HI-protocol for 5 to 10 weeks, and then cryopreserved in RecoveryTM Cell Culture Freezing Medium (GIBCO). They were shipped, thawed, and then further cultured for at least 5 weeks under the HI-protocol and then the methods were switched to the TMDU-protocol a week prior to transplantation. Acute colitis was induced by feeding *Rag2*$^{-/-}$ mice with 3.0% DSS (molecular weight 10,000; Ensuiko Sugar Refining Co.) dissolved in drinking water for 5 d (d 1 to 5). Body weights of the mice were monitored daily to evaluate the severity of colitis. 7 and 10 d after the start of DSS administration, the donor organoids were released from the type I collagen gel, dissociated by EDTA, and washed with BSA-containing PBS as with the passage procedure. Small clumps of cells equivalent to those from ~500 organoids were resuspended in 200 μl of a diluted Matrigel (1:20) in PBS. The cell suspension was instilled into colonic lumen by using a syringe and a thin flexible catheter 4 cm in length and 2 mm in diameter. After infusion, the anal verge was glued for 6 h to prevent luminal contents from being excreted immediately. After the transplantation on d 10, mice were maintained as usual before they were sacrificed and analyzed.

TRITC-Dextran Permeability Assay

Intestinal permeability was assessed by enteral administration of TRITC-dextran (molecular mass 4.4 kDa; Sigma), a nonmetabolizable macromolecule that is used as a permeability probe. Transplanted or sham-transplanted mice were gavaged with